© 2022. Published by The Company of Biologists Ltd | Journal of Experimental Biology (2022) 225, jeb244279. doi:10.1242/jeb.244279

RESEARCH ARTICLE

Characterization of two novel ammonia transporters, Hiat1a and Hiat1b, in the teleost model system *Danio rerio*

Haonan Zhouyao[1], Alex M. Zimmer[2,3], Sandra Fehsenfeld[4], Thomas Liebenstein[5], David O. Richter[5], Gerrit Begemann[5], Peter Eck[1], Steve F. Perry[3] and Dirk Weihrauch[6,*]

ABSTRACT

Ammonia excretion in fish excretory epithelia is a complex interplay of multiple membrane transport proteins and mechanisms. Using the model system of zebrafish (*Danio rerio*) larvae, here we identified three paralogues of a novel ammonia transporter, hippocampus-abundant transcript 1 (DrHiat1), also found in most vertebrates. When functionally expressed in *Xenopus laevis* oocytes, DrHiat1a and DrHiat1b promoted methylamine uptake in a competitive manner with ammonia. *In situ* hybridization experiments showed that both transporters were expressed as early as the 4-cell stage in zebrafish embryos and could be identified in most tissues 4 days post-fertilization. Larvae experiencing morpholino-mediated knockdown of DrHiat1b exhibited significantly lower whole-body ammonia excretion rates compared with control larvae. Markedly decreased site-specific total ammonia excretion of up to 85% was observed in both the pharyngeal region (site of developing gills) and the yolk sac (region shown to have the highest NH_4^+ flux). This study is the first to identify DrHiat1b/DrHIAT1 in particular as an important contributor to ammonia excretion in larval zebrafish. Being evolutionarily conserved, these proteins are likely involved in multiple other general ammonia-handling mechanisms, making them worthy candidates for future studies on nitrogen regulation in fishes and across the animal kingdom.

KEY WORDS: Morpholino, SIET, *In situ* hybridization, Zebrafish larvae

INTRODUCTION

Ammonia is a toxic waste product generated by the catabolism of proteins and nucleic acids, but also via ureolytic and uricolytic pathways (Larsen et al., 2014) (in the current study, NH_4^+ refers to the ammonium ion, NH_3 to gaseous ammonia, and ammonia to the sum of both). Ammonia is a weak base with a pK_a of 9.0–9.5 and occurs accordingly in physiological solutions predominantly (>90%) in its ionic form, NH_4^+, while only a small portion is present as the membrane-permeable NH_3 (Cameron and Heisler, 1983). In fishes, elevated plasma ammonia levels caused by exercise or feeding (Bucking, 2017; Fehsenfeld and Wood, 2018; Sinha et al., 2012a,b) need to be tightly regulated to avoid negative physiological implications. Furthermore, when exposed to non-lethal high environmental ammonia (HEA), the resulting internal plasma ammonia load can cause a wide range of deleterious effects in fish, including disruption of general ion homeostasis (Dircx et al., 2013; Wilkie, 1997), reduced swimming performance (McKenzie et al., 2009, 2003; Shingles et al., 2001), changes in energy metabolism (Arillo et al., 1981; Sinha et al., 2012a) and a reduced growth rate (Dosdat et al., 2003). To avoid its negative side effects, ammonia needs to be rapidly excreted from the body fluids. With a few exceptions, teleost fishes are ammoniotelic and excrete up to 90% of their metabolically produced ammonia directly through the gills (Sayer and Davenport, 1987; Smith et al., 2012; Smith, 1929; Zimmer et al., 2014).

In 2009, Wright and Wood (2009) published a working model for the branchial ammonia excretion mechanisms in a freshwater fish with the contribution of Rhesus-glycoproteins. It is assumed that plasma ammonia enters the epithelial cell in its gaseous form NH_3 via a basolateral localized Rhesus-glycoprotein, Rhbg, along its partial pressure gradient. Further, Mallery (1983) and Nawata et al. (2010) showed that similar to invertebrates (Adlimoghaddam et al., 2015; Hans et al., 2018; Masui et al., 2002) and the mammalian kidney (Wall and Koger, 1994), teleost Na^+/K^+-ATPase (NKA) is capable of accepting NH_4^+ instead of K^+ as a substrate. Consequently, in addition to NH_3 uptake via Rhbg, the basolateral NKA may mediate an active uptake of extracellular NH_4^+ into the branchial epithelial cell. The capacity of NKA to accept NH_4^+ as a substrate, however, seems to be dependent on external salinity and varies substantially among fishes (Wood and Nawata, 2011).

According to the model (Wright and Wood, 2009), it is further assumed that cytoplasmatic ammonia is excreted apically in a sodium-dependent manner via an apical Na^+/NH_4^+ exchange complex (Ito et al., 2013; Wright and Wood, 2009). This complex is thought to act as a metabolon that promotes the acidification of the unstirred boundary layer by means of a V-type H^+-ATPase and Na^+/H^+-exchanger 3 (NHE3), with both transporters creating a partial pressure gradient for gaseous NH_3. NH_3 follows this gradient utilizing another Rhesus-glycoprotein, Rhcgb (formerly Rhcg1; Nakada et al., 2007), a process commonly referred as ammonia trapping. A membrane-bound carbonic anhydrase (CA2a and/or CA15a; Ito et al., 2013) supports this metabolon by catalysing the hydration of CO_2, providing the required H^+ for the process (Wright and Wood, 2009). A similar ammonia excretion mechanism has also been proposed for freshwater planarians (Weihrauch et al., 2012). An equivalent mechanism, i.e. a sodium-dependent apical Na^+/NH_4^+ exchange metabolon, however, could not be verified for freshwater leeches, where the cutaneous ammonia excretion process was shown

[1]University of Manitoba, Department of Food and Human Nutritional Sciences, 66 Chancellors Circle, Winnipeg, MB, Canada, R3T 2N2. [2]University of Alberta, Department of Biological Science, 11355 Saskatchewan Drive, Edmonton, AB, Canada, T6G 2E9. [3]University of Ottawa, Department of Biology, 30 Marie Curie, Ottawa, ON, Canada, K1N 6N5. [4]Université du Quebec à Rimouski, Département de biologie, chimie et géographie, 300 Allée des Ursulines, Rimouski, QC, Canada, G5L 3A1. [5]Universität Bayreuth, Department of Biology, Universitätsstr. 30, University of Bayreuth, 95440 Bayreuth, Germany. [6]University of Manitoba, Department of Biological Sciences, 66 Chancellors Circle, Winnipeg, MB, Canada, R3T 2N2.

*Author for correspondence (dirk.weihrauch@umanitoba.ca)

S.F., 0000-0003-4495-8715; D.O.R., 0000-0001-6649-964X; G.B., 0000-0001-7822-7617; P.E., 0000-0003-2371-9774; D.W., 0000-0002-3218-9093

Received 16 March 2022; Accepted 7 September 2022

Journal of Experimental Biology (2022) 225, jeb244279. doi:10.1242/jeb.244279

to be independent of functional apical Na^+ channels and NHEs (Quijada-Rodriguez et al., 2017). Furthermore, in the nematode *Caenorhabditis elegans*, knock-out of the apically localized Rh-protein RHR-2 caused a reduction in ammonia excretion rates; the remaining flux was, however, independent of environmental pH, in contrast to the wild-type (Adlimoghaddam et al., 2016). However, in contrast to predictions stemming from the metabolon model (Wright and Wood, 2009), knocking out the apical Rhcgb in zebrafish via CRISPR/Cas9 did not reduce ammonia excretion and/or Na^+ uptake. Rather, an increase in ammonia excretion was observed (Zimmer and Perry, 2020). The diversity of ammonia excretory mechanisms across fishes and other aquatic animals underlies their importance for nitrogen homeostasis, and at the same time warrants the consideration of additional routes and mechanisms.

In invertebrates, for example, NH_4^+-transporting ammonium transporters (AMTs, also members of the AMT/MEP/Rh-protein ammonia transporter family), driven by the cytoplasm-to-environment electrochemical gradient of the cation, were suggested to be involved in the epithelial ammonia excretion process (clams: Boo et al., 2018; insects: Chasiotis et al., 2016; Durant and Donini, 2018; Pitts et al., 2014; polychaeta: Thiel et al., 2017). In vertebrates, however, AMTs have not been shown to be expressed to date.

An additional potential contributor to the branchial ammonia excretory process is the hippocampus-abundant transcript 1 protein (Hiat1). This presumptive ammonia transporter (CmHiat1) was associated with acid–base regulation in the green crab, *Carcinus maenas*, because its mRNA levels decreased when the animals were acclimated to elevated P_{CO_2} levels (Fehsenfeld et al., 2011). Recently, it was demonstrated that CmHiat1 acts as an ammonia (likely NH_4^+) transporter in this species (S.F., A. R. Quijada-Rodriguez, H.Z., A. C. Durant, A. Donini, M. Sachs, M. F. Romero, P.E. and D.W., unpublished) with its mRNA abundance found to be up-regulated in response to high environmental ammonia.

In light of the results of these studies, the current study was designed to test the hypothesis that Hiat1 is involved in ammonia excretion in zebrafish larvae. To address these hypotheses, we investigated Hiat1 function using multiple physiological and molecular techniques. After identifying and characterizing Hiat1 paralogues in a phylogenetic analysis, we expressed DrHiat1a and DrHiat1b proteins in frog oocytes to verify their capability to transport methylamine (ammonia analogue) competitively with NH_4Cl. We then determined mRNA expression patterns of both paralogues throughout early development (4-cell stage to 4 days post-fertilization) by *in situ* hybridization. Lastly, we knocked down DrHiat1a and DrHiat1b using morpholino injections and applied the scanning ion-selective electrode technique (SIET) to identify regions of interest of Hiat1-related ammonia flux in *D. rerio* larvae in early development.

MATERIALS AND METHODS

Sequence-based genetic structure analysis

DrHiat1-like (GenBank accession no. XP_002663499.2; 500 amino acids), DrHiat1b (GenBank accession no. AAH97075.1, 485 amino acids) and the translated DrHiat1a protein based on the open reading frame (ORF) of zebrafish *DrHiat1a* (GenBank accession no. BC056817, 493 amino acids) were aligned with Clustal Omega (https://www.ebi.ac.uk/Tools/msa/clustalo/). Protter (Omasits et al., 2014) was used to predict transmembrane (TM) domains and the potential phosphorylation sites for all three Hiat1 proteins, and Scansite 4.0 (Obenauer et al., 2003) was used to identify the binding motifs. All transmembrane models and proteoform predictions were performed using the system's default settings.

DrHiat1b was then used to identify Hiat1 isoforms in other species via GenBank-BLASTp search (Table S1) (Altschul et al., 1997). Proteins were aligned with the MUSCLE algorithm as provided by the Molecular Evolutionary Genetics Analysis across computing platforms (MEGA X; Kumar et al., 2018) using default settings. The evolutionary history was inferred by using the Maximum Likelihood method and JTT matrix-based model (Jones et al., 1992) as identified by the testing function provided by MEGA X. Initial trees for the heuristic search were obtained automatically by applying Neighbor-Join and BioNJ algorithms to a matrix of pairwise distances estimated using a JTT model, and then selecting the topology with superior log-likelihood value. A discrete Gamma distribution was used to model evolutionary rate differences among sites [5 categories (+G, parameter=0.3614)]. All positions with less than 95% site coverage were eliminated, i.e. fewer than 5% alignment gaps, missing data and ambiguous bases were allowed at any position (partial deletion option).

Heterologous expression of *DrHiat1a* and *DrHiat1b* in *Xenopus* oocytes

cDNA clones containing the full ORFs of *DrHiat1a* (clone ID: 2640969; GenBank accession number BC056817.1) and *DrHiat1b* (clone ID: 2600163, GenBank accession number BC097075) were purchased from Dharmacon (Lafayette, CO, USA). DNA miniprep kits (Qiagen, Hilden, Germany) were used to extract the plasmids following the manufacturer's guidance. Regular PCR employing Q5 High-Fidelity DNA Polymerase was used to obtain the full ORFs of *DrHiat1a* and *DrHiat1b* (see Table S2, ORF). The annealing temperature used for the amplification of *DrHiat1a* and *DrHiat1b* ORFs was 60°C and 62°C, respectively, with a total of 35 cycles. Subsequently, regular PCR was used to add restriction enzyme sites to the 5′ and 3′ ends of the ORFs of *DrHiat1a* and *DrHiat1b* (see Table S2, oocytes). The annealing temperature used for the amplification of *DrHiat1a* and *DrHiat1b* ORFs was 65°C for both, with a total of 35 cycles. The quality of the DNA was assessed by gel electrophoresis and the concentration of DNA was determined spectrophotometrically after purification (GeneJET PCR purification kit, ThermoFisher, Waltham, MA, USA). The ORFs were then cloned into the pGEM®-HE plasmid, a modified pGEM®-3Z vector containing the *Xenopus* beta globin 5′- and 3′-UTR sequences, using T4 ligase following the manufacturer's guidance [New England Biolabs (NEB), Ipswich, MA, USA]. The *in vitro* transcription of capped mRNA (cRNA) was performed with HiScribe™ T7 ARCA mRNA kit (NEB) followed by column purification (RNeasy MinElute Cleanup Kit, Qiagen). The cRNA was quantified spectrophotometrically (Nanodrop, ND-1000, ThermoFisher) and integrity was assessed on a Mops agarose gel containing formaldehyde.

Stage VI–V oocytes were collected from mature female *Xenopus laevis* (VWR, Radnor, PA, USA) as previously described (Soreq and Seidman, 1992) (Protocol Reference F20-021). Briefly, the frogs were euthanized via decapitation prior to ovary collection. The ovary was placed in Ca^{2+}-free OR2 solution (in mmol l^{-1}: 82.5 NaCl, 2.5 KCl, 1 $MgCl_2$, 1 Na_2HPO_4, 5 Hepes; pH 7.2) with collagenase type VI (1 mg ml^{-1}) (Gibco, Waltham, MA, USA) and gently agitated for 90 min at room temperature; 1 mmol l^{-1} $CaCl_2$ was added to terminate the collagenase activity. Oocytes were then manually sorted and rinsed three additional times with standard OR2 solution. For overnight storage of isolated oocytes, OR2 was supplemented with 2.5 mmol l^{-1} sodium pyruvate, 1 mg ml^{-1} penicillin–streptomycin (Gibco, Long Island, NY, USA) and 50 µg ml^{-1} gentamicin at 16°C. All procedures used were

Journal of Experimental Biology (2022) 225, jeb244279. doi:10.1242/jeb.244279

approved by the University of Manitoba Animal Research Ethics Board and are in accordance with the Guidelines of the Canadian Council on Animal Care.

Isolated oocytes after the overnight recovery were injected with 18.4 ng of cRNA (36.8 nl with 0.5 ng nl^{-1}) or nuclease-free water as control using a Nanoject II auto-nanolitre injector (Drummond Scientific, Broomall, PA, USA). Experiments were conducted 48 h post-injection.

[H^3]Methylamine transport studies in oocytes expressing DrHiat1a and DrHiat1b

[H^3]Methylamine uptake experiments

Experiments were conducted at room temperature in 200 µl of standard OR2 solution, containing 3 µmol l^{-1} (9.3 µCi) [H^3]methylamine (Moravek Inc., Brea, CA, USA) with 60 min of incubation time. For each experiment 20 oocytes injected with either with cRNA or water (sham) were randomly selected. At the end of each experiment, ice-cold standard OR2 solution was used to terminate [H^3]methylamine uptake by washing oocytes 3 times to remove the external radioactivity. The washed oocytes were immediately solubilized individually in 200 µl of 10% SDS (Sigma-Aldrich, St Louis, MO, USA) to assess the internal radioactivity, employing 5 ml of Ultima-Gold scintillation cocktail (PerkinElmer) and liquid scintillation counting (Tri-Carb 2900 TR; PerkinElmer). The effect of washing was determined by assessing the radioactivity in 200 µl standard OR2 solution used for the third wash post-radioactivity exposure compared with fresh, radioactivity-free standard OR2 solution of the same volume. For NH_4Cl competitive uptake experiments, the same procedures described above were conducted, but with 1 mmol l^{-1} NH_4Cl added to the incubation solution.

[H^3]Methylamine release experiments

To determine whether Hiat proteins mediate bi-directional methylamine transport, the efflux of methylamine from sham oocytes, and from DrHiat1a- and DrHiat1b-expressing oocytes was measured. Experiments were performed at room temperature in 200 µl of standard OR2 solution containing 3 µmol l^{-1} (9.3 µCi) [H^3]methylamine adjusted to pH 7.2, with 60 min incubation time. Two groups of cRNA-injected oocytes (n=20) and two groups of water-injected oocytes (sham; n=20) were assessed for each experimental point. Each group was considered as one replicate and, overall, two replicates were done. After termination of [H^3]methylamine uptake as described above, one group of cRNA-injected oocytes and one group of water-injected oocytes were immediately solubilized individually to assess the uptake of [H^3]methylamine as described above, to determine the starting point for the following release experiment. The remaining groups of cRNA-injected oocytes and water-injected oocytes were placed in 200 µl of room temperature, radioactivity-free standard OR2 solution for 60 min for release and afterwards washed 3 times with ice-cold standard OR2 solution, solubilized individually in 200 µl of 10% SDS and assessed for remaining internal radioactivity. The efficiency of the washing steps was determined by analysing 200 µl of the radioactivity of the third wash post-radioactivity exposure compared with that of fresh, radioactivity-free standard OR2 solution of the same volume.

In situ hybridization

DrHiat1a and *DrHiat1b* ORFs were amplified and cloned as described above with Q5 High Fidelity DNA Polymerase (NEB) and primers located at both ends of the ORFs with restriction enzyme sites (Table S2, *In situ*).

The deletion of the *Xenopus* beta-globin 5′-UTR was done by removing a 63 bp fragment containing the 5′-UTR with KpnI and XmaI followed by blunting with Quick Blunting Kit (NEB) and re-ligation. The *Xenopus* beta-globin 3′-UTR was removed in the course of linearization of the vector for the preparation of an antisense RNA probe. The antisense RNA probe was synthesized as previously described (Thisse and Thisse, 2008) and experiments were conducted at the University of Bayreuth, Germany, using the Casper strain (White et al., 2008). Adult fish were maintained under standard conditions (14 h:10 h light:dark cycle; 0.1 g l^{-1} salinity; 300 µS conductivity; pH 7.5) at 27.5–28.5°C. Embryos were obtained from pairing events of 3 male and 2 female fish and were reared in E3-medium (in mmol l^{-1}: 5 NaCl, 0.17 KCl, 0.33 $CaCl_2$, 0.33 $MgSO_4$, 10.5% Methylene Blue; pH 7.2) at 28.5°C.

Zebrafish embryos and larvae were euthanized on ice, fixed in 4% PFA/PBS, washed in PBS/0.1% Tween 20 (PBTw), transferred to 100% methanol and stored at least overnight at −20°C. After rehydration using a methanol/PBTw series and post-fixation in 4% PFA/PBS, older developmental stages were treated with 10 µg ml^{-1} proteinase K (Fermentas, Waltham, MA, USA) for 10 min (2 days post-fertilization, dpf), 15 min (3 dpf) and 20 min (4 dpf), post-fixed in 4% PFA/PBS and washed several times in PBTw. After hybridization with the corresponding antisense probes overnight at 68°C, the samples were washed in a formamide solution/PBTw series, blocked in 0.5% blocking reagent, incubated in a 1:2000 dilution of anti-DIG-AP antibody in 0.5% blocking reagent for 4 h at room temperature and washed several times in PBTw. For detection, samples were equilibrated in BCL buffer and stained with NBT and BCIP/X-phos until staining was clearly visible.

Ammonia excretion studies in zebrafish with *DrHiat1a* or *DrHiat1b* knockdown

Zebrafish

Danio rerio (F. Hamilton 1822) originally purchased from the pet trade (Big Al's Aquarium, Ottawa, ON, Canada) were maintained in flow-through aquaria receiving dechlorinated city of Ottawa tap water ('system water'; in mmol l^{-1}: 0.8 Na^+, 0.4 Cl^-, 0.25 Ca^{2+}; pH 7.6) and held at 28.5°C with a 14 h:10 h light:dark photoperiod. Embryos were obtained from breeding events between 1 male and 2 females held in static tanks, and reared in 60 ml Petri dishes containing system water with 0.05% Methylene Blue at a density of approximately 50 embryos per dish held at 28°C. Handling and experimentation of zebrafish was conducted in compliance with the University of Ottawa Animal Care and Veterinary Service (ACVS) guidelines under protocol BL-1700 and followed the recommendations from the Canadian Council for Animal Care (CCAC).

Morpholino injections

Splice-blocking morpholino oligonucleotides (Gene Tools, LLC, Philomath, OR, USA) targeting the intron–exon junction between intron and exon 4 of *DrHiat1a* (NCBI accession no.: NM_199584.1; 5′-CATGGTGAGAGCCTCTGAAATCAAG-3′) and the intron–exon junction between intron and exon 4 of *DrHiat1b* (NCBI accession no.: NM_213527.2; 5′-AAAGTGAGGAGCGTAAC-GAACCATG-3′), and a standard control morpholino with no biological target in zebrafish (5′-CCTCTTACCTCAGTTACAATT-TATA-3′) were suspended to a final concentration of 2–4 ng morpholino nl^{-1} in Danieau buffer [in mmol l^{-1}: 58 NaCl, 0.7 KCl, 0.4 $MgSO_4$, 0.6 $Ca(NO_3)_2$, and 5.0 Hepes buffer; pH 7.6] containing 0.05% Phenol Red for injection visualization. One-cell stage embryos were injected with 1 nl of this injection solution

Journal of Experimental Biology (2022) 225, jeb244279. doi:10.1242/jeb.244279

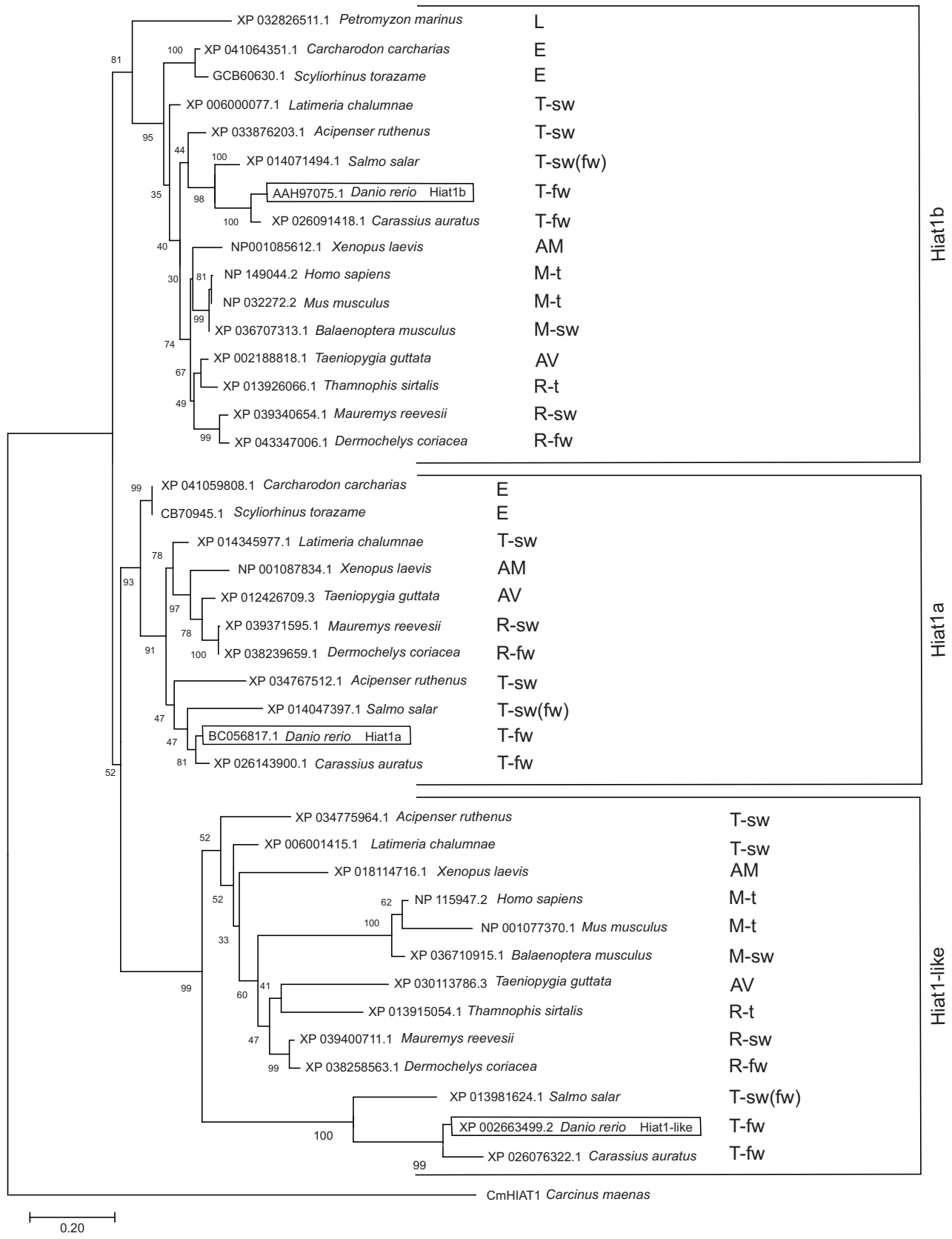

Fig. 1. See next page for legend.

[4 ng per embryo for *DrHiat1a* morpholino (MO), 4 ng per embryo for *DrHiat1b* MO, and 4 ng per embryo for control (sham) MO] using an IM 300 microinjection system (Narishige, Amityville, NY, USA). However, we observed a large proportion (>50%) of morphological abnormalities (curved tail/spine) with the 4 ng *DrHiat1b* dose and therefore used a dose of 2 ng for *DrHiat1b* and

Fig. 1. Phylogenetic analysis of Hiat1-like, Hiat1a and Hiat1b across vertebrates. The maximum likelihood consensus tree of the MUSCLE alignment (Edgar, 2004) of Hiat1 proteins as performed with MEGAX (Kumar et al., 2018). Numbers beside branches represent bootstrap values (1000 replicates). The tree is drawn to scale, with branch lengths measured in the number of substitutions per site (indicated by the bar at the bottom). AM, Amphibia; AV, Aves; E, Elasmobranchii; L, lamprey; M-sw, marine Mammalia; M-t, terrestrial Mammalia; R-fw, freshwater Reptilia; R-sw, seawater Reptilia; R-t, terrestrial Reptilia, T-fw, freshwater Teleostei; T-sw, seawater Teleostei. *Salmo salar* is indicated as both marine and freshwater as it returns to freshwater for reproduction. The tree was rooted by including the recently identified Hiat-protein in the green crab, *Carcinus maenas* (S.F., A. R. Quijada-Rodriguez, H.Z., A. C. Durant, A. Donini, M. Sachs, M. F. Romero, P.E. and D.W., unpublished).

observed virtually no morphological abnormalities (<5–10%). Injections were verified at 1 dpf by examining the distribution of carboxyfluorescein (tagged to each morpholino) in individual embryos under a fluorescence dissecting microscope (Nikon SMZ1500, Nikon Instruments, Melville, NY, USA). Embryos that were successfully injected, containing a homogeneous distribution of fluorescein signal, were reared as described above.

Knockdown was confirmed by reverse transcription PCR (RT-PCR). At 4 dpf, approximately 20 pooled larvae (n=1) from each treatment group (*DrHiat1a* MO, *DrHiat1b* MO and sham MO) were euthanized by an overdose of neutralized tricaine methanesulfonate (MS-222; Syndel Canada, Nanaimo, BC, Canada), flash frozen in liquid nitrogen, and stored at −80°C. RNA was extracted from pooled samples using Trizol (ThermoFisher) following the manufacturer's protocol. Extracted RNA was treated with DNAse (ThermoFisher) and cDNA was then synthesized from 700 ng total RNA using the iScript cDNA synthesis kit (Bio-Rad, Hercules, CA, USA). PCR was performed using DreamTaq DNA polymerase (ThermoFisher) following the manufacturer's guidance, with primers specific to *DrHiat1a* and *DrHiat1b* (see Table S2). The reaction volume for each PCR reaction was 20 µl with 55°C annealing temperature and the reaction was terminated after 40 cycles.

Whole-body ammonia flux

At 4 dpf, *DrHiat1a*, *DrHiat1b* and sham MO-treated larvae were placed into 2 ml centrifuge tubes containing 1.5 ml system water (6 larvae per tube; n=1) maintained at 28–30°C in a water bath. Larvae were allowed to adjust for 30 min; thereafter, initial 0.5 ml water samples were drawn from each tube, marking the beginning of the flux period. Following a 6 h flux period, final 0.5 ml water samples were drawn from each tube. Samples were frozen and stored at −20°C for no longer than 1 week. Total ammonia concentration (T_{Amm}) was measured using the indophenol method (Verdouw et al., 1978) and ammonia excretion rate (nmol larva^{-1} h^{-1}) was calculated using the following equation:

$$\text{Ammonia excretion} = [(T_{Amm,f} - T_{Amm,i}) \times V]/t/n, \quad (1)$$

where $T_{Amm,f}$ and $T_{Amm,i}$ (nmol ml^{-1}) are the final and initial total ammonia concentrations, respectively, V is volume (ml), t is flux duration (h) and n is the number of larvae in the tube.

SIET

SIET was performed to assess NH_4^+ flux in sham and *DrHiat1b* MO-treated 4 dpf larvae. Measurements were made in a K^+-free medium which was prepared by adding stock solutions of Na_2SO_4, $CaCl_2$, $MgSO_4{\cdot}7H_2O$, Na_2HPO_4 and NaH_2PO_4 to doubly distilled water (in mmol l^{-1}: 0.84 Na^+, 0.5 Cl^-, 0.25 Ca^{2+}, 0.15 Mg^{2+}; pH 7.6). The omission of K^+ in the medium is necessary because this ion interferes with NH_4^+ signals from the ion-selective probe. In addition, the medium contained MS-222 anaesthetic (0.2 g l^{-1}) and 0.05 mmol l^{-1} $(NH_4)_2SO_4$, the latter being necessary because the Nernstian slope of NH_4^+ tends to fall at concentrations below 0.1 mmol l^{-1}.

NH_4^+-selective probes were constructed as described previously (Donini and O'Donnell, 2005). Glass capillary tubes (World Precision Instruments, Sarasota, FL, USA) were pulled to microelectrodes with a tip diameter of approximately 5 µm using a P-2000 micropipette puller (Sutter Instrument, Novato, CA, USA) and silanized with *N*,*N*-dimethyltrimethylsilylamine (Sigma-Aldrich) on a hot plate covered with a glass Petri dish. Silanized microelectrodes were then back-loaded with 100 mmol l^{-1} NH_4Cl and front-loaded with an approximately 250 µl ionophore column of NH_4^+ Ionophore I Cocktail A (Sigma-Aldrich). Probes were calibrated in the same K^+-free medium containing MS-222 described above to which NH_4Cl was added to a final concentration of 0.1, 1 or 10 mmol l^{-1}. pH was maintained at 7.6 across all calibration solutions using NaOH or H_2SO_4. The slope (in mV) for a tenfold change in NH_4^+ concentration was 59.2±1.1 (n=3).

Larvae were allowed to adjust to the measurement solution for 15–20 min prior to flux measurements; thereafter, they were restrained in a measurement chamber described previously (Hughes et al., 2019) that prevented larvae from drifting during measurements. NH_4^+ flux was measured at the apex of the yolk sac epithelium, similar to previous studies (Shih et al., 2012) and at the pharyngeal region, the latter measurement being used as an approximation of gill NH_4^+ flux. Voltage from the NH_4^+-selective probe was measured approximately 2–5 µm away from the epithelial surface (origin) and at an excursion distance of 100 µm away from the epithelium (excursion). Each scan consisted of 5 replicate origin and extrusion measurements and scans were replicated 3 times at the yolk sac and at the jaw for each fish (n=1). For each fish, a background scan was conducted at the beginning and end of the measurement at a location approximately 1 cm away from the larva. Voltage gradients were converted to concentration gradients using the following equation (Donini and O'Donnell, 2005):

$$\Delta C = C_B \times 10^{(\Delta V/S)} - C_B, \quad (2)$$

where ΔC is the concentration gradient (µmol cm^{-3}) between the origin and excursion points, C_B is the average background ion concentration measured by the probe at all points, ΔV is the voltage difference (mV) between the origin and excursion points, and S is the slope obtained from the probe calibration (mV). Note that ΔV of the background solution was subtracted from that measured at the epithelium. Flux was then calculated using Fick's law of diffusion:

$$J = D \times \Delta C/\Delta x, \quad (3)$$

where J is NH_4^+ flux (pmol cm^{-2} s^{-1}), D is the diffusion coefficient for NH_4^+ (2.09×10^{-5} cm^2 s^{-1}) and Δx is the excursion distance (cm).

Statistics

All data were tested for normal distribution by Shapiro–Wilk's test. In cases where data were not normally distributed, data were log transformed. Homogeneity of variances was assessed by Levene's test. If data did not meet the criteria for parametric testing including normal distribution and homogeneity of variances, non-parametric test were applied. Statistical analyses were performed with PAST3 (Hammer et al., 2001). Graphs were generated with GraphPad Prism

Journal of Experimental Biology (2022) 225, jeb244279. doi:10.1242/jeb.244279

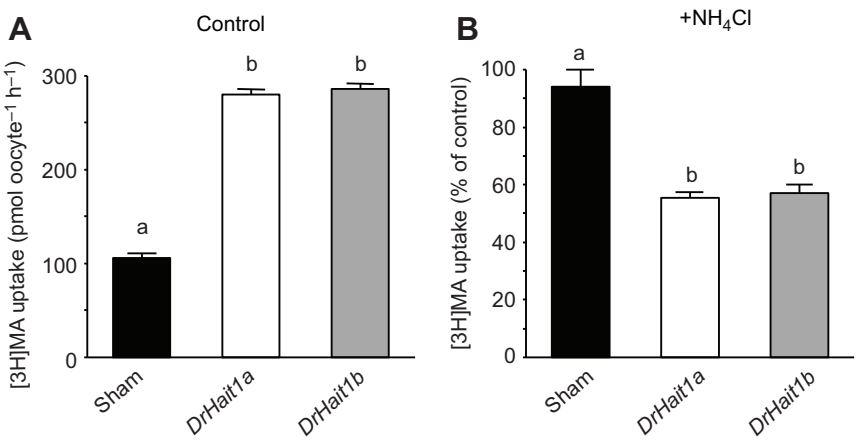

Fig. 2. DrHiat1a and DrHiat1b-mediated methylamine/methylammonium uptake in *Xenopus laevis* oocytes. (A) Absolute [^{3}H]methylamine/methylammonium (MA) uptake of sham-injected oocytes (black) and oocytes expressing DrHiat1a (white) or DrHiat1b (grey) under control conditions (medium pH 7.2). (B) Relative [^{3}H]MA uptake of sham-injected oocytes (black) and oocytes expressing DrHiat1a (white) or DrHiat1b (grey) in medium containing 1 mmol l^{-1} NH_4Cl. Values are depicted as a percentage of the corresponding control values as shown in A. Data are means+s.e.m. Different letters indicate significant differences as identified with one-way ANOVA and Tukey's *post hoc* test (P<0.001, N=19, 20, 20).

9.0 for Windows (GraphPad Software, San Diego, CA, USA; www.graphpad.com) and Inkscape (https://inkscape.org).

RESULTS

Genetic analysis of Hiat1

The three isoforms of DrHiat1 are referred to as DrHiat1a, DrHiat1b and Hiat1-like according to the current nomenclature used by GenBank. DrHiat1a (493 amino acids), DrHiat1b (485 amino acids) and DrHiat1-like (500 amino acids) exhibited a conservation of 323 identical amino acids (ca. 66%), with 80 residues as strongly conserved groups (two out of three amino acids identical; ca. 16%) and 19 residues as weakly conserved groups (three different amino acids but with similar properties; ca. 4%). The structure analysis of DrHiat1a, DrHiat1b and DrHiat1-like by Protter (Omasits et al., 2014) identified 12 predicted TM domains. Furthermore, a sugar binding motif (amino acids 91–108 for DrHiat1a, amino acids 89–106 for DrHiat1b, amino acids 103–120 for Hiat1-like) seems to be associated with TM3 in all three cases. While DrHiat1a and DrHiat1b contained two equivalent phosphoserine/threonine binding groups (amino acids 5–21/amino acids 5–19, N-terminal; amino acids 299–312/amino acids 297–310, between TM8 and TM9) (Larner et al., 1993), DrHiat1b contained an additional one between TM1 and TM2 (amino acids 55–70), but DrHiat1-like did not contain any at all. DrHiat1b was the only isoform to contain a proline-dependent serine/threonine kinase group (Lew et al., 1992; Meyerson et al., 1992) (Cdk5, amino acids 456–469) (Fig. S1).

Our preliminary phylogenetic analysis showed Hiat1 to be conserved across many taxa and clustered in three distinct clades according to the three different paralogues (Fig. 1).

DrHiat1-mediated methylamine transport in *Xenopus laevis* oocytes

Both DrHiat1a and DrHiat1b-expressing oocytes showed significantly higher (2.7-fold) methylamine (MA) uptake compared with the sham (oocytes injected with water, negative control). There was no difference in the uptake of MA between oocytes expressing DrHiat1a or DrHiat1b (Fig. 2A; ANOVA with Tukey's pairwise comparisons with P<0.001, N=20).

When exposed to 1 mmol l^{-1} non-labelled NH_4Cl in addition to MA in the medium, the uptake of MA mediated by DrHiat1a and DrHiat1b was reduced by 45% and 40%, respectively. The degree of inhibition of MA by NH_4Cl was not significantly different between oocytes expressing DrHiat1a and DrHiat1b (Fig. 2B).

Pre-loaded DrHiat1a- and DrHiat1b-expressing oocytes released significantly more ammonia compared with sham-injected oocytes (27% versus 15%; Fig. 3). There was no difference between the amount of MA released in oocytes expressing Hiat1a and Hiat1b.

In situ hybridization of Hiat1 isoforms in zebrafish embryos and larvae

To determine Hiat1 expression in zebrafish, *DrHiat1a* and *DrHiat1b* antisense RNA probes were generated and whole-mount *in situ* hybridization (WISH) was performed on zebrafish embryos and larvae of different developmental stages, beginning from the 4-cell stage until 4 dpf (Fig. 4). This revealed maternal expression of both *DrHiat1a* (Fig. 4Ai) and *DrHiat1b* (Fig. 4Bi), early onset of transcription during the maternal-to-zygotic transition (Fig. 4Ai′ and Bi′) and ubiquitous expression in all tissues during early segmentation stages (Fig. 4Aii,ii′,Bii,ii′). At 24 h post-fertilization (hpf), towards the end of the segmentation period, expression of both genes was mainly localized to the head region, especially to the forebrain, midbrain and hindbrain, including the midbrain–hindbrain boundary, the lens and the trigeminal ganglion (Fig. 4Aiii,iii′,Biii,iii′). In addition, *DrHiat1a* showed distinct expression in the olfactory placode and the hatching gland in both examined segmentation stages (Fig. 4Aii,ii′,iii,iii′), while *DrHiat1b* showed additional expression in the optic vesicle, posterior lateral

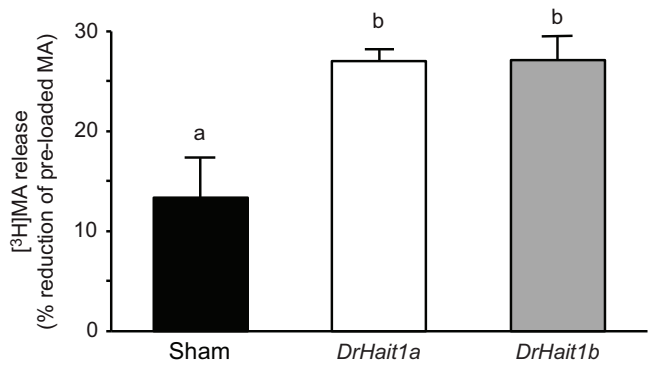

Fig. 3. Relative MA release of pre-loaded *X. laevis* oocytes expressing DrHiat1a or DrHiat1b. Oocytes were pre-loaded in MA-containing medium for 60 min after which internal oocyte MA concentration was measured (MA_{pre}). Subsequently, oocytes were transferred to MA-free medium and MA concentration was re-measured after an additional 60 min (MA release, MA_{rel}). The graph shows the MA release relative to pre-loaded values calculated as MA release=100%−(MA_{rel}/MA_{pre}×100%). Data are means+s.e.m. Different letters indicate significant differences as identified by Kruskal–Wallis test with Mann–Whitney pairwise and Bonferroni-corrected comparisons (P<0.03, N=20, 20, 20).

Journal of Experimental Biology (2022) 225, jeb244279. doi:10.1242/jeb.244279

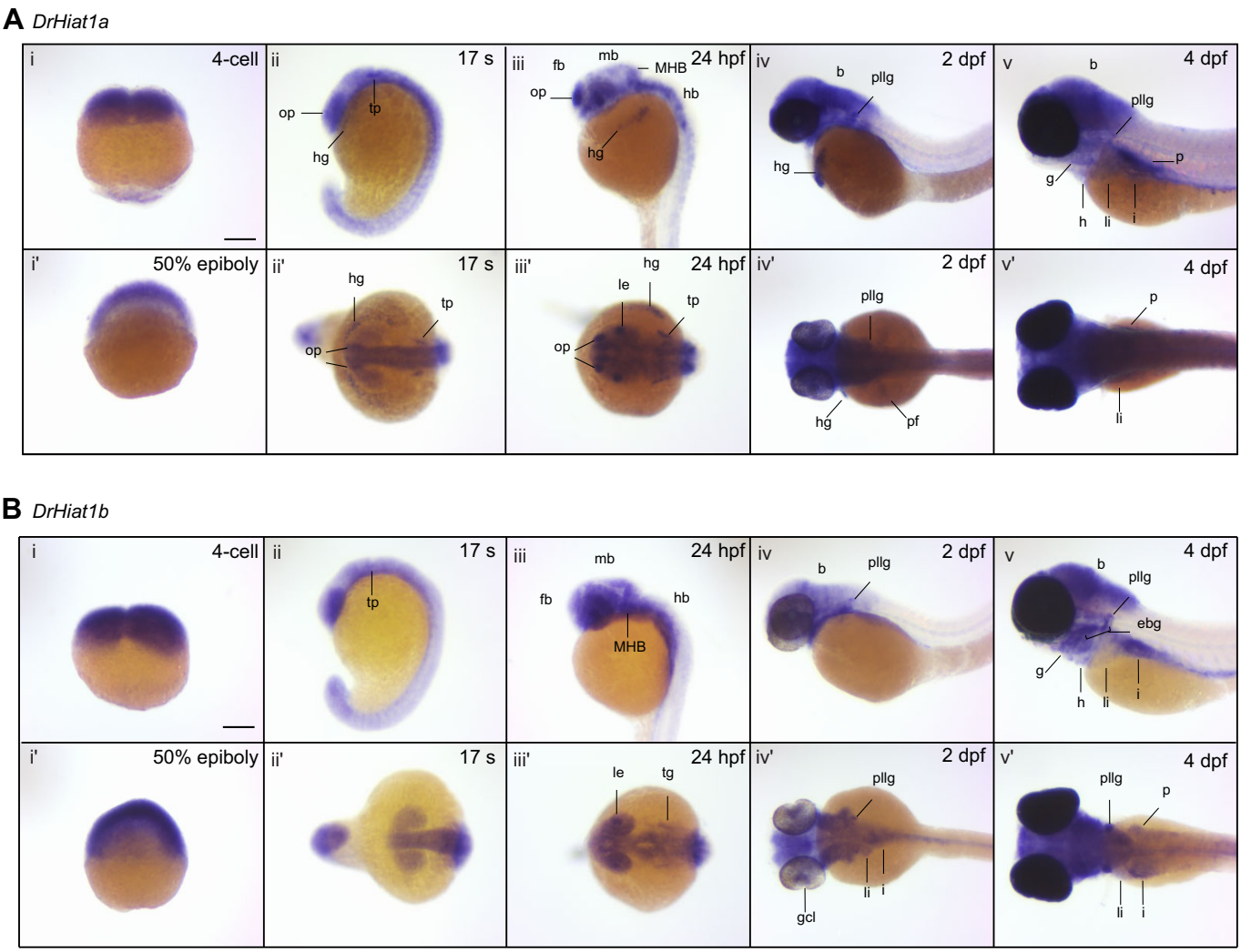

Fig. 4. Expression pattern of *DrHiat1a* and *DrHiat1b* in zebrafish embryos and larvae during early development. Whole-mount *in situ* hybridization of *DrHiat1a* (A) and *DrHiat1b* (B) at the 4-cell stage, 50% maternal-to-zygotic transition (50% epiboly), 17 somite stage (17 s), 24 h post-fertilization (hpf) and 2/4 days post-fertilization (dpf). i,i′: lateral view, animal pole to the top; ii–v: lateral view, anterior to the left; ii′–v′: dorsal view, anterior to the left. b, brain; fb, forebrain; g, gills; h, heart; hb, hindbrain; hg, hatching gland; i, intestine; le, lens; li, liver; mb, midbrain; MHB, midbrain–hindbrain boundary; op, olfactory placode; p, pancreas; pf, pectoral fin; pllg, posterior lateral line ganglion; tg, trigeminal ganglion; tp, trigeminal placode. Scale bar (for all images): 200 µm.

line ganglion and pectoral fin bud at 24 hpf (see Fig. S1). From 2 to 4 dpf, *DrHiat1a* and *DrHiat1b* expression could be detected in the brain, heart, gills, digestive system, pectoral fins and parts of the sensory nervous system including the cranial and lateral line ganglia (*DrHiat1a* and *DrHiat1b*) and the retinal ganglion cell layer and lateral line neuromasts (*DrHiat1b*) (Fig. 4Aiv,iv′,v,v′,Biv,iv′, v,v′; Fig. S1). For the digestive system, *DrHiat1a* appeared to be more strongly expressed in the pancreas, whereas *DrHiat1b* was more apparent in the intestine (Fig. S1E–H). Because of the proteinase K treatment, which was performed from 2 dpf onwards, staining of some of the more external structures, such as the pectoral fins and lateral line neuromasts, was reduced or even completely abolished. For images without proteinase K treatment, see Fig. S2.

Ammonia excretion in zebrafish larvae with *DrHiat1* knockdown

Successful knockdown of *Hiat1a* and *Hiat1b* using splice-blocking MOs was verified by PCR, where the reduced size of amplicons (from 450 to 300 bp) indicates successful splice blocking of the 4th exon in pre-mRNA *DrHiat1a* and *DrHiat1b* such that the respective exon was not included in mature mRNA (Fig. 5A).

A significant reduction of ammonia excretion was found in larvae with *DrHiat1b* knockdown, but not with *DrHiat1a* knockdown (Fig. 5B). SIET was then used to measure the regional flux of NH_4^+ on larvae with *DrHiat1b* knockdown (Fig. 6A). NH_4^+-selective electrodes were placed at the yolk sac and pharyngeal region/immature gill region (Fig. 6A). A significant reduction of NH_4^+ flux was detected at both regions in *DrHiat1b* knockdown larvae compared with the sham larvae (Fig. 6B).

DISCUSSION

Despite their high level of sequence conservation (86%), Hiat1a, Hiat1b, Hiat1-like transporters (renamed mfsd14a/b in mammals; Doran et al., 2016; Lekholm et al., 2017) could be clearly distinguished in the phylogenetic analysis. Unfortunately, likely as a result of the high level of amino acid similarity and the lack of research on the phylogeny and function of these transporters, there is currently no consistent nomenclature available in the literature and databases. Consequently, the reader needs to be aware that many

Journal of Experimental Biology (2022) 225, jeb244279. doi:10.1242/jeb.244279

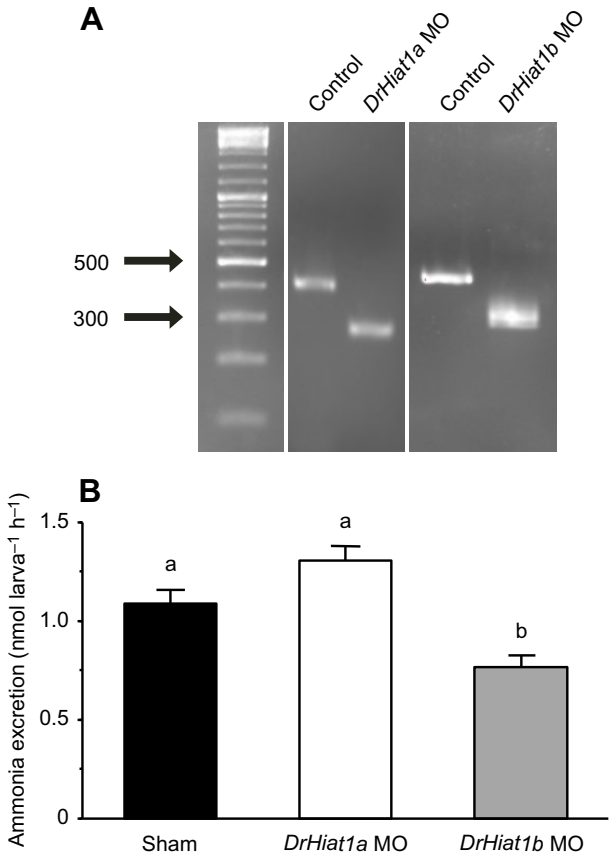

Fig. 5. Whole-animal ammonia excretion in *DrHiat1a* and *DrHiat1b* knock-down larvae. (A) Confirmation of successful *DrHiat1a*/*DrHiat1b* knockdown (morpholinos, MO) in 4 dpf larvae, indicated by a reduced size of PCR products compared with control, caused by blockage of pre-mRNA splicing in the MOs. (B) Ammonia excretion in sham-injected larvae and *DrHiat1a*/*DrHiat1b* knockdown larvae (MOs). Data are means+s.e.m. Different letters indicate significant differences as identified by Kruskal–Wallis test with Mann–Whitney pairwise and Bonferroni-corrected comparisons (P<0.004, N=41, 24, 29).

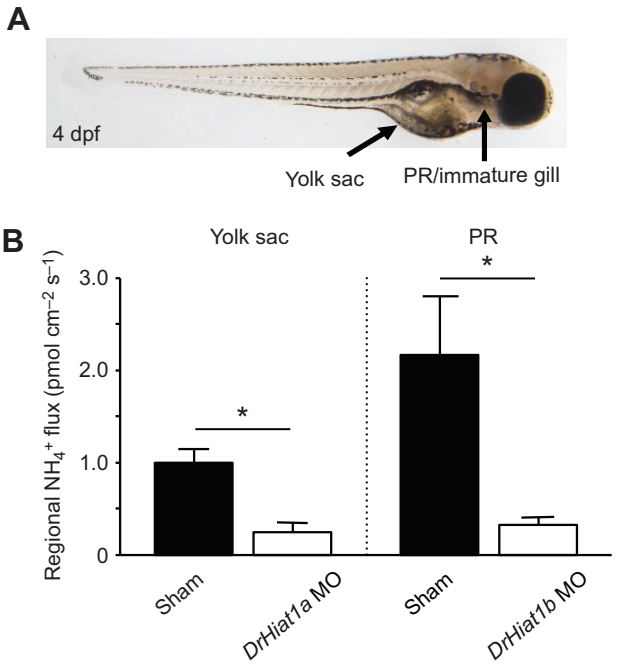

Fig. 6. Regional NH_4^+ flux in *DrHiat1b* knock-down larvae. (A) Microelectrodes were placed at the yolk sac and pharyngeal region (PR)/immature gill of larvae 4 dpf. (B) The scanning ion-selective micro-electrode technique (SIET) was used to measure NH_4^+ at these distinct regions in sham and *DrHiat1b* MO larvae. Data are means+s.e.m. Asterisks denote significant differences as identified with Student's *t*-test (P<0.004, N=4–7 animals per condition and site).

proteins annotated as one or the other in the NCBI database did not hold true in our analysis (i.e. many transcripts annotated as Hiat1-like instead cluster as Hiat1b or Hiat1a). It should also be noted that some sequences that were annotated as different isoforms turned out to be simply truncated/not properly assembled versions of the same gene. We therefore present here a potential reference for future annotations of this transporter based on the zebrafish names for each of the *Hiat1* paralogues.

To date, only one isoform of Hiat1 has been identified in invertebrates (S.F., A. R. Quijada-Rodriguez, H.Z., A. C. Durant, A. Donini, M. Sachs, M. F. Romero, P.E. and D.W., unpublished). Interestingly, while all three isoforms can be identified in teleosts, other vertebrates seem to lack one or more: for lamprey, only Hiat1b could be identified, Hiat1-like was not found for elasmobranchs, and no Hiat1a was identified for terrestrial reptilians as well as terrestrial and aquatic mammals. At this point, further phylogenetic analysis would be needed to clarify the exact evolutionary history of the different isoforms.

Zebrafish Hiat1a and Hiat1b as novel ammonia transporters

The present study revealed that both DrHiat1a and DrHiat1b could promote MA uptake when expressed in frog oocytes. Furthermore, MA release was enhanced in pre-loaded oocytes when expressing either of the *Hiat1* paralogues. Adding the fact that external ammonia was able to inhibit MA uptake in transgenic oocytes (as seen by the immediate inhibition of MA uptake in the presence of NH_4Cl in the medium) allows us to conclude that DrHiat1a and DrHiat1b also function as ammonia transporters. An equivalent observation was made in our recent study (S.F., A. R. Quijada-Rodriguez, H.Z., A. C. Durant, A. Donini, M. Sachs, M. F. Romero, P.E. and D.W., unpublished) in green crabs, where CmHiat1 promoted ammonium transport (likely NH_4^+), shown either directly with scanning ion-selective microelectrodes, or indirectly with radiolabelled MA as a proxy. Despite possessing a sugar transporter-specific motif D-R/K-X-G-R-R/K between TM domain 2 and TM domain 3 (Matsuo et al., 1997), recent results clearly showed a lack of glucose transport in *X. laevis* oocytes when expressing crustacean Hiat1 (S.F., A. R. Quijada-Rodriguez, H.Z., A. C. Durant, A. Donini, M. Sachs, M. F. Romero, P.E. and D.W., unpublished). Similarly, mammalian Mfsd14a was not capable of mediating glucose uptake into the oocyte (Zhouyao et al., 2022).

Interestingly, competition of NH_4^+ transport with MA uptake was only observed in transgenic oocytes, but barely in sham-injected oocytes. This might simply be based on the respective concentration of NH_4^+ (1 mmol l^{-1}): competition might occur at higher concentrations of NH_4^+ as the kinetics of ammonia/MA transport by endogenous pathways in *Xenopus* oocytes may just have a much higher inhibition constant. Or, in other words, MA uptake by DrHiat1 may have a lower inhibition constant than the endogenous pathways for ammonia uptake of the *Xenopus* oocytes (i.e. via Rhesus-glycoproteins and/or NHE3), such that we saw this large difference at 1 mmol l^{-1} NH_4Cl.

Hiat1b-mediated ammonia excretion in zebrafish larvae

Ammonia handling and excretion seem to be especially important in early life stages of fish for a variety of reasons. First, because of an

amino acid-focused metabolism, the ammonia load in fish embryos is substantial (Zimmer et al., 2017). Second, embryos experience physiological constraints; these include the presence of a chorion capsule as a barrier that impedes diffusion between the embryo and its external environment, and the lack of fully functional gills which function as the main ammonia excretory organ in more mature fish (Zimmer et al., 2017).

Generally, ammonia excretion in larval zebrafish occurs in part via H^+-ATPase-rich (HR) cells in the yolk sac and gills that also contain apical Rhesus-glycoprotein 1 (Rhcg1 or Rhcgb) (Nakada et al., 2007), NHE3 (Ito et al., 2013) and H^+-ATPase (Lin et al., 2006). Furthermore, with their unique expression patterns along the skin, gills and yolk sac, Rhag, Rhbg, Rhcg1 (Rhcgb) and Rhcg2 (Rhcgl1) have all been shown to contribute to whole zebrafish larvae ammonia excretion to varying extents (Braun et al., 2009; Zimmer and Perry, 2020). Additionally, Rhbg and/or Rhcg1 (Rhcgb) also seem to more specifically participate in the excretion of ammonia via skin keratinocytes (Shih et al., 2008, 2013). In contrast, a Na^+/NH_4^+ exchange metabolon as mentioned in the Introduction, seems instead to contribute to ammonia excretion only under challenging conditions (i.e. low pH and/or low Na^+ environments) and less so when fish were kept in unaltered laboratory conditions (i.e. circumneutral water with adequate salt concentrations) (Kumai and Perry, 2011; Shih et al., 2012).

Here, we provide the first evidence that ammonia excretion in this early life stage appears to be additionally mediated by DrHiat1b, hence giving an alternative route for basic ammonia transport. Interestingly, *Hiat1* is expressed in frog oocytes and hence maternally provided (S.F., A. R. Quijada-Rodriguez, H.Z., A. C. Durant, A. Donini, M. Sachs, M. F. Romero, P.E. and D.W., unpublished), ensuring it is passed on with the maternal lineage, implying a crucial role for this transporter as early as development begins. The fact that both *DrHiat1a* and *DrHita1b* are ubiquitously expressed in the zebrafish embryo and early larvae emphasizes their importance as potential ammonia transporters in this crucial phase of life. They might provide a very general route for baseline ammonia excretion in every tissue, complemented by more differentially expressed and tissue-specific Rhesus-glycoproteins. It is not surprising that both *Hiat1* transcripts can initially be found in the nervous system, resembling the first discovery of *Hiat* in the marsupial hippocampus (Matsuo et al., 1997). *DrHiat1b* being more abundantly expressed might indicate its more important role for basic ammonia maintenance and might also explain the subtle differences in tissue expression. For instance, while mRNA for *DrHiat1b* was present in the intestine, mRNA for *DrHiat1a* was not detectable.

In *DrHiat1b* MO knockdowns, whole-larvae ammonia excretion was reduced by ca. 30%. The fact that we observed an even further reduction of ammonia excretion when we specifically screened the yolk sac (−75%) and pharyngeal region (immature gill; −85%) underlines the complexity of excretory mechanisms in this stage. Similar discrepancies have been observed in earlier studies on zebrafish larvae, when for example, Zimmer and Perry (2020) found that a knockdown of Rhcgb resulted in an increase of whole-larvae ammonia excretion, whereas NH_4^+ flux at the yolk sac assessed by SIET was reduced in response to knockdown using the same MO (Shih et al., 2008; 2012). Further thorough investigations are needed to fully understand these respective mechanisms, including potential off-target effects and/or compensatory responses caused by knockdown, i.e. the possibility that other ammonia transporters such as Rhesus-glycoproteins take over after the loss of Hiat1 (Kok et al., 2015; Rossi et al., 2015).

Conclusion

The findings of the present study warrant a reconsideration of ammonia-related transport processes in the gills and potentially other excretory organs of fish. We show here that especially early on in development, the involvement of Hiat1b and/or Hiat1a provides an alternative route for ammonia transport besides the involvement of Rhesus-glycoproteins and/or Na^+/NH_4^+ exchange metabolon. Alternatively, Hiat1a/1b could be part of this metabolon. It would be highly desirable for future studies to identify the transporters' exact cellular localization in the branchial membrane to allow for more detailed modelling of branchial ammonia transport. Clearly, Hiat1 transporters have to be taken into account in future studies on ammonia transport in fish and other animals, including the mammalian kidney.

Acknowledgements

We like to thank the Animal Care and Veterinary Services at the University of Ottawa, and in particular Christine Archer and Vishal Saxena for taking care of the zebrafish.

Competing interests

The authors declare no competing or financial interests.

Author contributions

Conceptualization: D.W.; Methodology: H.Z., A.M.Z., S.F., T.L., D.O.R., G.B., D.W.; Validation: D.W.; Formal analysis: A.M.Z., S.F.; Investigation: H.Z., A.M.Z., T.L., D.O.R., G.B.; Resources: D.W.; Writing - original draft: H.Z.; Writing - review & editing: A.M.Z., S.F., D.O.R., G.B., S.P., D.W.; Supervision: P.E., S.P., D.W.; Project administration: D.W.; Funding acquisition: P.E., S.P., D.W.

Funding

Financial support was provided by Natural Sciences and Engineering Research Council of Canada Discovery grants (NSERC RGPIN-5013–2018 to D.W., RGPIN-2018-06027 to P.E., and NSERC G13017 to S.P.). The research was further supported by a University of Manitoba UCRP grant (2017-18/SUB 318995) to D.W. and P.E. H.Z. was awarded a Company of Biologists travel grant for this collaboration. S.F. and A.Z. are/were the recipients of a Natural Sciences and Engineering Research Council of Canada postdoctoral fellowship.

References

Adlimoghaddam, A., Boeckstaens, M., Marini, A. M., Treberg, J. R., Brassinga, A. K. C. and Weihrauch, D. (2015). Ammonia excretion in *Caenorhabditis elegans*: mechanism and evidence of ammonia transport of the Rhesus protein CeRhr-1. *J. Exp. Biol.* **218**, 675-683. doi:10.1242/jeb.111856

Adlimoghaddam, A., O'Donnell, M. J., Kormish, J., Banh, S., Treberg, J. R., Merz, D. and Weihrauch, D. (2016). Ammonia excretion in *Caenorhabditis elegans*: physiological and molecular characterization of the rhr-2 knock-out mutant. *Comp. Biochem. Physiol. A Mol. Integr. Physiol.* **195**, 46-54. doi:10.1016/j.cbpa.2016.02.003

Altschul, S. F., Madden, T. L., Schäffer, A. A., Zhang, J., Zhang, Z., Miller, W. and Lipman, D. J. (1997). Gapped BLAST and PSI-BLAST: a new generation of protein database search programs. *Nucleic Acids Res.* **25**, 3389-3402. doi: 10.1093/nar/25.17.3389

Arillo, A., Margiocco, C., Melodia, F., Mesi, P. and Schenone, G. (1981). Ammonia toxicity mechanism in fish: studies on rainbow trout *(Salmo gairdneri* Rich). *Ecotoxicol. Environ. Saf.* **5**, 316-328. 10.1016/0147-6513(81)90006-3

Boo, M. V., Hiong, K. C., Goh, E. J. K., Choo, C. Y. L., Wong, W. P., Chew, S. F. and Ip, Y. K. (2018). The ctenidium of the giant clam, *Tridacna squamosa*, expresses an ammonium transporter 1 that displays light-suppressed gene and protein expression and may be involved in ammonia excretion. *J. Comp. Physiol. B Biochem. Syst. Environ. Physiol.* **188**, 765-777. doi:10.1007/s00360-018-1161-6

Braun, M. H., Steele, S. L., Ekker, M. and Perry, S. F. (2009). Nitrogen excretion in developing zebrafish (*Danio rerio*): a role for Rh proteins and urea transporters. *Am. J. Physiol. Renal Physiol.* **296**, F994-F1005. doi:10.1152/ajprenal.90656.2008

Bucking, C. (2017). A broader look at ammonia production, excretion, and transport in fish: a review of impacts of feeding and the environment. *J. Comp. Physiol. B* **187**, 1-18. doi:10.1007/s00360-016-1026-9

Cameron, J. N. and Heisler, N. (1983). Studies of ammonia in the rainbow trout: physico-chemical parameters, acid-base behaviour and respiratory clearance. *J. Exp. Biol.* **105**, 107-125. Retrieved from http://jeb.biologists.org/content/105/1/107.short. doi:10.1242/jeb.105.1.107

Chasiotis, H., Ionescu, A., Misyura, L., Bui, P., Fazio, K., Wang, J., Weihrauch, D. and Donini, A. (2016). An animal homolog of plant Mep/Amt transporters promotes ammonia excretion by the anal papillae of the disease vector mosquito *Aedes aegypti*. *J. Exp. Biol.* **219**, 1346-1355. doi:10.1242/jeb.134494

Diricx, M., Sinha, A. K., Liew, H. J., Mauro, N., Blust, R. and De Boeck, G. (2013). Compensatory responses in common carp (*Cyprinus carpio*) under ammonia exposure: additional effects of feeding and exercise. *Aquat. Toxicol.* **142-143**, 123-137. doi:10.1016/j.aquatox.2013.08.007

Donini, A. and O'Donnell, M. J. (2005). Analysis of Na^+, Cl^-, K^+, H^+ and NH_4^+ concentration gradients adjacent to the surface of anal papillae of the mosquito *Aedes aegypti*: application of self-referencing ion-selective microelectrodes. *J. Exp. Biol.* **208**, 603-610. doi:10.1242/jeb.01422

Doran, J., Walters, C., Kyle, V., Wooding, P., Hammett-burke, R. and Colledge, W. H. (2016). *Mfsd*14*a* (*Hiat*1) gene disruption causes globozoospermia and infertility in male mice. *Reproduction* **152**, 91-99. doi:10.1530/REP-15-0557

Dosdat, A., Ruyet, J. P.-L., Coves, D., Dutto, G., Gasset, E., Le Roux, A. and Lemarie, G. (2003). Effect of chronic exposure to ammonia on growth, food utilisation and metabolism of the European sea bass (*Dicentrarchus labrax*). *Aquat. Living Resour.* **16**, 509-520. doi:10.1016/j.aquliv.2003.08.001

Durant, A. C. and Donini, A. (2018). Ammonia excretion in an osmoregulatory syncytium is facilitated by AeAmt2, a novel ammonia transporter in *Aedes aegypti* larvae. *Front. Physiol.* **9**, 339. doi:10.3389/fphys.2018.00339

Edgar, R. C. (2004). MUSCLE: a multiple sequence alignment method with reduced time and space complexity. *BMC Bioinformatics* **5**, 113. doi:10.1186/1471-2105-5-113

Fehsenfeld, S. and Wood, C. M. (2018). Section-specific expression of acid-base and ammonia transporters in the kidney tubules of the goldfish *Carassius auratus* and their responses to feeding. *Am. J. Physiol. Renal Physiol.* **315**, F1565-F1582. doi:10.1152/ajprenal.00510.2017

Fehsenfeld, S., Kiko, R., Appelhans, Y. S., Towle, D. W., Zimmer, M. and Melzner, F. (2011). Effects of elevated seawater pCO_2 on gene expression patterns in the gills of the green crab, *Carcinus maenas*. *BMC Genomics* **12**, 488. doi:10.1186/1471-2164-12-488

Hammer, Ø., Harper, D. A. T. and Ryan, P. D. (2001). PAST: paleontological statistics software package for education and data analysis. *Palaeontol. Electron.* **4**, 1-9.

Hans, S., Quijada-Rodriguez, A. R., Allen, G. J. P., Onken, H., Treberg, J. R. and Weihrauch, D. (2018). Ammonia excretion and acid-base regulation in the American horseshoe crab, *Limulus polyphemus*. *J. Exp. Biol.* **221**, jeb151894. doi:10.1242/jeb.151894

Hughes, M. C., Zimmer, A. M. and Perry, S. F. (2019). Role of internal convection in respiratory gas transfer and aerobic metabolism in larval zebrafish (*Danio rerio*). *Am. J. Physiol. Regul. Integr. Comp. Physiol.* **316**, R255-R264. doi:10.1152/ajpregu.00315.2018

Ito, Y., Kobayashi, S., Nakamura, N., Miyagi, H., Esaki, M., Hoshijima, K. and Hirose, S. (2013). Close association of carbonic anhydrase (CA2a and CA15a), Na^+/H^+ exchanger (Nhe3b), and ammonia transporter Rhcg1 in zebrafish ionocytes responsible for Na^+ uptake. *Front. Physiol.* **4**, 59. doi:10.3389/fphys.2013.00059

Jones, D. T., Taylor, W. R. and Thornton, J. M. (1992). The rapid generation of mutation data matrices from protein sequences. *Comput. Appl. Biosci.* **8**, 275-282. doi:10.1093/bioinformatics/8.3.275

Kok, F. O., Shin, M., Ni, C. W., Gupta, A., Grosse, A. S., VanImpel, A., Kirchmaier, B. C., Peterson-Maduro, J., Kourkoulis, G. and Male, I. (2015). Reverse genetic screening reveals poor correlation between morpholino-induced and mutant phenotypes in zebrafish. *Dev. Cell* **32**, 97-108. doi:10.1016/j.devcel.2014.11.018

Kumai, Y. and Perry, S. F. (2011). Ammonia excretion via Rhcg1 facilitates Na^+ uptake in larval zebrafish, *Danio rerio*, in acidic water. *Am. J. Physiol. Regul. Integr. Comp. Physiol.* **301**, R1517-R1528. doi:10.1152/ajpregu.00282.2011

Kumar, S., Stecher, G., Li, M., Knyaz, C. and Tamura, K. (2018). MEGA X: molecular evolutionary genetics analysis across computing platforms. *Mol. Biol. Evol.* **35**, 1547-1549. doi:10.1093/molbev/msy096

Larner, A. C., David, M., Feldman, G. M., Igarashi, K. I., Hackett, R. H., Webb, D. S. A., Sweitzer, S. M., Petricoin, E. F. and Finbloom, D. S. (1993). Tyrosine phosphorylation of DNA binding proteins by multiple cytokines. *Science* **261**, 1730-1733. doi:10.1126/science.8378773

Larsen, E. H., Deaton, L. E., Onken, H., O'Donnell, M., Grosell, M., Dantzler, W. H. and Weihrauch, D. (2014). Osmoregulation and excretion. *Compr. Physiol.* **4**, 405-573. doi:10.1002/cphy.c130004

Lekholm, E., Perland, E., Eriksson, M. M., Hellsten, S. V., Lindberg, F. A., Rostami, J. and Fredriksson, R. (2017). Putative membrane-bound transporters MFSD14A and MFSD14B are neuronal and affected by nutrient availability. *Front. Mol. Neurosci.* **10**, 11. doi:10.3389/fnmol.2017.00011

Lew, J., Beaudette, K., Litwin, C. M. E. and Wang, J. H. (1992). Purification and characterization of a novel proline-directed protein kinase from bovine brain. *J. Biol. Chem.* **267**, 13383-13390. doi:10.1016/s0021-9258(18)42222-3

Lin, L. Y., Horng, J. L., Kunkel, J. G. and Hwang, P. P. (2006). Proton pump-rich cell secretes acid in skin of zebrafish larvae. *Am. J. Physiol. Cell Physiol.* **290**, 371-378. doi:10.1152/ajpcell.00281.2005

Mallery, C. H. (1983). A carrier enzyme basis for ammonium excretion in teleost gill. NH_4^+-stimulated Na-dependent ATPase activity in *Opsanus beta*. *Comp. Biochem. Physiol. A Physiol.* **74**, 889-897. doi:10.1016/0300-9629(83)90364-X

Masui, D. C., Furriel, R. P. M., McNamara, J. C., Mantelatto, F. L. M. and Leone, F. A. (2002). Modulation by ammonium ions of gill microsomal (Na^+,K^+)-ATPase in the swimming crab *Callinectes danae*: a possible mechanism for regulation of ammonia excretion. *Comp. Biochem. Physiol. C Toxicol. Pharmacol.* **132**, 471-482. doi:10.1016/S1532-0456(02)00110-2

Matsuo, N., Kawamoto, S., Matsubara, K. and Okubo, K. (1997). Cloning of a cDNA encoding a novel sugar transporter expressed in the neonatal mouse hippocampus. *Biochem. Biophys. Res. Commun.* **238**, 126-129. doi:10.1006/bbrc.1997.7252

McKenzie, D. J., Shingles, A. and Taylor, E. W. (2003). Sub-lethal plasma ammonia accumulation and the exercise performance of salmonids. *Comp. Biochem. Physiol. A Mol. Integr. Physiol.* **135**, 515-526. doi:10.1016/S1095-6433(03)00116-8

Mckenzie, D. J., Shingles, A., Claireaux, G. and Domenici, P. (2009). Sublethal concentrations of ammonia impair performance of the teleost fast-start escape response. *Physiol. Biochem. Zool.* **82**, 353-362. doi:10.1086/590218

Meyerson, M., Enders, G. H., Wu, C.-L., Su, L.-K., Gorka, C., Nelson, C., Harlow, E. and Tsai, L.-H. (1992). A family of human cdc2-related protein kinases. *EMBO J.* **11**, 2909-2917. doi:10.1002/j.1460-2075.1992.tb05360.x

Nakada, T., Hoshijima, K., Esaki, M., Nagayoshi, S., Kawakami, K. and Hirose, S. (2007). Localization of ammonia transporter Rhcg1 in mitochondrion-rich cells of yolk sac, gill, and kidney of zebrafish and its ionic strength-dependent expression. *Am. J. Physiol. Regul. Integr. Comp. Physiol.* **293**, R1743-R1753. doi:10.1152/ajpregu.00248.2007

Nawata, C. M., Hirose, S., Nakada, T., Wood, C. M. and Kato, A. (2010). Rh glycoprotein expression is modulated in pufferfish (*Takifugu rubripes*) during high environmental ammonia exposure. *J. Exp. Biol.* **213**, 3150-3160. doi:10.1242/jeb.044719

Obenauer, J. C., Cantley, L. C. and Yaffe, M. B. (2003). Scansite 2.0: proteome-wide prediction of cell signalling interactions using short sequence motifs. *Nucleic Acids Res.* **31**, 3635-3641. doi:10.1093/nar/gkg584

Omasits, U., Ahrens, C. H., Mu, S. and Wollscheid, B. (2014). Sequence analysis Protter: interactive protein feature visualization and integration with experimental proteomic data. *Bioinformatics* **30**, 884-886. doi:10.1093/bioinformatics/btt607

Pitts, R. J., Derryberry, S. L., Pulous, F. E. and Zwiebel, L. J. (2014). Antennal-expressed ammonium transporters in the malaria vector mosquito *Anopheles gambiae*. *PLoS One* **9**, e111858. doi:10.1371/journal.pone.0111858

Quijada-Rodriguez, A. R., Schultz, A. G., Wilson, J. M., He, Y., Allen, G. J. P., Goss, G. G. and Weihrauch, D. (2017). Ammonia-independent sodium uptake mediated by Na^+ channels and NHEs in the freshwater ribbon leech *Nephelopsis obscura*. *J. Exp. Biol.* **220**, 3270-3279. doi:10.1242/jeb.159459

Rossi, A., Kontarakis, Z., Gerri, C., Nolte, H., Hölper, S., Krüger, M. and Stainier, D. Y. R. (2015). Genetic compensation induced by deleterious mutations but not gene knockdowns. *Nature* **524**, 230-233. doi:10.1038/nature14580

Sayer, M. D. J. and Davenport, J. (1987). The relative importance of the gills to ammonia and urea excretion in five seawater and one freshwater teleost species. *J. Fish Biol.* **31**, 561-570. doi:10.1111/j.1095-8649.1987.tb05258.x

Shih, T.-H., Horng, J.-L., Hwang, P.-P. and Lin, L.-Y. (2008). Ammonia excretion by the skin of zebrafish (*Danio rerio*) larvae. *Am. J. Physiol. Cell Physiol.* **295**, C1625-C1632. doi:10.1152/ajpcell.00255.2008

Shih, T.-H., Horng, J.-L., Liu, S.-T., Hwang, P.-P. and Lin, L.-Y. (2012). Rhcg1 and NHE3b are involved in ammonium-dependent sodium uptake by zebrafish larvae acclimated to low-sodium water. *Am. J. Physiol. Regul. Integr. Comp. Physiol.* **302**, R84-R93. doi:10.1152/ajpregu.00318.2011

Shih, T.-H., Horng, J.-L., Lai, Y.-T. and Lin, L.-Y. (2013). Rhcg1 and Rhbg mediate ammonia excretion by ionocytes and keratinocytes in the skin of zebrafish larvae: H^+-ATPase-linked active ammonia excretion by ionocytes. *Am. J. Physiol. Regul. Integr. Comp. Physiol.* **304**, R1130-R1138. doi:10.1152/ajpregu.00550.2012

Shingles, A., McKenzie, D. J., Taylor, E. W., Moretti, A., Butler, P. J. and Ceradini, S. (2001). Effects of sublethal ammonia exposure on swimming performance in rainbow trout (*Oncorhynchus mykiss*). *J. Exp. Biol.* **204**, 2691-2698. doi:10.1242/jeb.204.15.2691

Sinha, A. K., Liew, H. J., Diricx, M., Blust, R. and De Boeck, G. (2012a). The interactive effects of ammonia exposure, nutritional status and exercise on metabolic and physiological responses in gold fish (*Carassius auratus* L.). *Aquat. Toxicol.* **109**, 33-46. doi:10.1016/j.aquatox.2011.11.002

Sinha, A. K., Liew, H. J., Diricx, M., Kumar, V., Darras, V. M., Blust, R. and De Boeck, G. (2012b). Combined effects of high environmental ammonia, starvation and exercise on hormonal and ion-regulatory response in goldfish (*Carassius auratus* L.). *Aquat. Toxicol.* **114-115**, 153-164. doi:10.1016/j.aquatox.2012.02.027

Smith, H. W. (1929). The excretion of ammonia and urea by the gills of fish. *J. Biol. Chem.* **81**, 727-742. doi:10.1016/s0021-9258(18)63725-1

Smith, A. A., Zimmer, A. M. and Wood, C. M. (2012). Branchial and extra-branchial ammonia excretion in goldfish (*Carassius auratus*) following thermally induced gill

remodeling. *Comp. Biochem. Physiol. A* **162**, 185-192. doi:10.1016/j.cbpa.2012.02.019

Soreq, H. and Seidman, S. (1992). [14]Xenopus oocyte microinjection: From gene to protein. *Methods in Enzymology* **207**, 225-265.

Thiel, D., Hugenschutt, M., Meyer, H., Paululat, A., Quijada-Rodriguez, A. R., Purschke, G. and Weihrauch, D. (2017). Ammonia excretion in the marine polychaete *Eurythoe complanata* (Annelida). *J. Exp. Biol.* **220**, 425-436. doi:10.1242/jeb.145615

Thisse, C. and Thisse, B. (2008). High-resolution in situ hybridization to whole-mount zebrafish embryos. *Nat. Protoc.* **3**, 59-69. doi:10.1038/nprot.2007.514

Verdouw, H., Van Echteld, C. J. A. and Dekkers, E. M. J. (1978). Ammonia determination based on indophenol formation with sodium salicylate. *Water Res.* **12**, 399-402. doi:10.1016/0043-1354(78)90107-0

Wall, S. M. and Koger, L. M. (1994). NH_4^+ transport mediated by Na^+-K^+-ATPase in rat inner medullary collecting duct. *Am. J. Physiol. Renal Physiol.* **267**, F660-F670. doi:10.1152/ajprenal.1994.267.4.f660

Weihrauch, D., Chan, A. C., Meyer, H., Döring, C., Sourial, M. and O'Donnel, M. J. (2012). Ammonia excretion in the freshwater planarian *Schmidtea mediterranea*. *J. Exp. Biol.* **215**, 3242-3253. doi:10.1242/jeb.067942

White, R. M., Sessa, A., Burke, C., Bowman, T., LeBlanc, J., Ceol, C., Bourque, C., Dovey, M., Goessling, W. and Burns, C. E. (2008). Transparent adult zebrafish as a tool for in vivo transplantation analysis. *Cell Stem Cell* **2**, 183-189. doi:10.1016/j.stem.2007.11.002

Wilkie, M. P. (1997). Mechanisms of ammonia excretion across fish gills. *Comp. Biochem. Physiol. A Physiol.* **118A**, 39-50. doi:10.1016/S0300-9629(96)00407-0

Wood, C. M. and Nawata, C. M. (2011). A nose-to-nose comparison of the physiological and molecular responses of rainbow trout to high environmental ammonia in seawater versus freshwater. *J. Exp. Biol.* **214**, 3557-3569. doi:10.1242/jeb.057802

Wright, P. A. and Wood, C. M. (2009). A new paradigm for ammonia excretion in aquatic animals: role of Rhesus (Rh) glycoproteins. *J. Exp. Biol.* **212**, 2303-2312. doi:10.1242/jeb.023085

Zhouyao, H., Fehsenfeld, S., Weihrauch, D. and Eck, K. P. (2022). The murine major facilitator superfamily domain containing 14A (*Mfsd*14*a*) gene does not encode a glucose transporter. *Adv. Nutr. Food Sci.* **2022**, 1-13. doi:10.37722/ANAFS.2022101

Zimmer, A. M. and Perry, S. F. (2020). The Rhesus glycoprotein Rhcgb is expendable for ammonia excretion and Na^+ uptake in zebrafish (*Danio rerio*). *Comp. Biochem. Physiol. A Mol. Integr. Physiol.* **247**, 110722. doi:10.1016/j.cbpa.2020.110722

Zimmer, A. M., Brauner, C. J. and Wood, C. M. (2014). Ammonia transport across the skin of adult rainbow trout (*Oncorhynchus mykiss*) exposed to high environmental ammonia (HEA). *J. Comp. Physiol. B Biochem. Syst. Environ. Physiol.* **184**, 77-90. doi:10.1007/s00360-013-0784-x

Zimmer, A. M., Wright, P. A. and Wood, C. M. (2017). Ammonia and urea handling by early life stages of fishes. *J. Exp. Biol.* **220**, 3843-3855. doi:10.1242/jeb.140210

```
                                                                        TM1
DrHiat1a       ------------MTGEKKKKKRLNRSILLAKKIIIKDGGTPQGIGEPSVYHAVVVIFLEF 48
DrHiat1b       --------------MTQKKKKRVNRSLLLAKKIIIKDGGTPQGFGSPSVYHAVIVIFLEF 46
DrHiat-like    MRCNDEMAMKMMMAQGEKDPKHTSRVVLVKRIIMKHDNPVQQGIGKPSVYHAVVVIFLEF 60
                                :*. *: .* :*: : *: :*. . **:*.*******:******
                  TM1                         TM2                    TM3
DrHiat1a       FAWGLLTTPMLAVLRQTFPQHTFLMNGLIHGVKGLLSFLSAPLIGALSDVWGRKSFLLLT 108
DrHiat1b       FAWGLLTAPTLGALDETFPKHTFLMNGLIQGVKGLLSFLSAPLIGALSDVWGRKSFLLLT 106
DrHiat-like    FAWGLLTTPMLTVLHETFPTHTFLINGLIQGVKGLLSFMSAPLIGALSDVWGRRSFLLVT 120
               *******:* * .* :*** ****:****:********:**************:****:*
                  TM3                   TM4                         TM5
DrHiat1a       VFFTCAPIPLMKISPWWYFAVISMSGVFAVTFSVIFAYVADITQEHERSTAYGLVSATFA 168
DrHiat1b       VFFTCAPIPLMKISPWWYFAMISVSGVFAVTFSVIFAYVADITQEHERSMAYGMVSATFA 166
DrHiat-like    VFFTCAPIPLMRLSPWWYFAMISVSGAFSVTFSVIFAYIADVTDERERSTAYGLVSATFA 180
               ***********::*******:**:**.*:*********:**:*:*:*** ***:******
                  TM5                     TM6
DrHiat1a       ASLVTSPAIGAYLSEVYGDTLVVILATAIALLDICFILVAVPESLPEKMRPASWGAPISW 228
DrHiat1b       ASLVISPAIGAYLSHVYGDTLVVVLASAIAMLDICLILVAVPESLPEKMRPASWGAPISW 226
DrHiat-like    ASLVTSPAIGAYLSASYGDNLVVLVATLIALADICFILLAVPESLPDKMRLNTWGAPISW 240
               **** *********  ***.***::*: **: ***:**:*******:***  :*******
                                          TM7                         TM8
DrHiat1a       EQADPFASLRKVGQDSTVLLICITVFLSYLPEAGQYSSFFLYLRQVIGFTSETVAAFIAV 288
DrHiat1b       EQADPFASLRKVGQDSTVLLICITVFLSYLPEAGQNSSFFLYLQQIMGFSSESVAAFIAV 286
DrHiat-like    EQADPFASLRKVGQDTTVLLICITVFLSYLPEAGQYSSFFLYLRQVINFSPKTIAVFIGV 300
               ***************:****************** *******:*::.*: :::*.**.*
                  TM8                        TM9                  TM10
DrHiat1a       VGILSILAQTVVLGILMRSIGNKNTILLGLGFQILQLAWYGFGSQPWMMWAAGAVAAMSS 348
DrHiat1b       LGLLSVVAQTVVLSLLMRSIGNKNTILLGLGFQILQLAWYGFGSEPWMMWAAGAVAAMSS 346
DrHiat-like    VGILSILAQTLFLTLLMRTIGNKNTVLLGLGFQILQLAWYGLGSEPWMMWAAGAVAAMSS 360
               :*:**::***:.* :***:******:***************:**:**************
                TM10                          TM11
DrHiat1a       ITFPAISAIVSRNADPDQQGVVQGMITGIRGLCNGLGPALYGFVFYLFHVELSEMDPAES 408
DrHiat1b       ITFPAVSALISRTADPDQQGVGQGMVTGIRGLCNGLGPALYGFIFYIFHVELDKVPEK-G 405
DrHiat-like    ITFPAVSALVSRSADPDKQGLVQGMITGIRGLCNGLGPALYGFVFFLFNVELSGITPIQ- 419
               *****:**::**.****:**: ***:*****************:*::*:***. :
                                          TM12
Hiat1a         PEKGVKPNMANPTDESAIIPGPPFLFGACSVLLSLLVALFIPEHNGLNLRPGSYKKHNNG 468
Hiat1b         PDV---QHHRDLHQQSAIIPGPPFLFGACSVLLALLVALFIPEHPHMGTRSGSWKHHTSP 462
Hiat-like      PDFAIP---IQTPTEKTTIPGPPFLLGACTVVVAFIVALFIPDHSTPPSTPCQTR-KNSL 475
                *:        :   :.: *******:***:*::::******:*         . : :..

Hiat1a         AQSHSHSSQGGQCEGKEPLLEDSSV 493
Hiat1b         HG-HPHS-PHPPGEAKEPLLQDTNV 485
Hiat-like      AGAHTNTPLPGSDEDFEPLLEDSTV 500
                  * ::      *  ****:*:.*
```

FIG S1

Fig. S1. Alignment of the three *Danio rerio* Hiat1 isoforms. Sequences for DrHiat1-like (GenBank accession number XP_002663499.2), DrHiat1a (GenBank acc. no. BC056817.1) and DrHiat1b (GenBank acc. no. AAH97075.1) were aligned with Clustal Omega (https://www.ebi.ac.uk/Tools/msa/clustalo/). Shown are the sugar biding motif in red letters, transmembrane domains in bold and underlined (TMs), Phosphoserine/threonine binding groups in light blue (Neck1) / purple (Neck2) / yellow (Neck6) and a proline-dependent serine/threonine kinase group in green (cyclin-dependent kinase 5 Cdk5). Asterisks denote conserved sites, ":" denote conserved strong groups and "." denote conservation of weak groups.

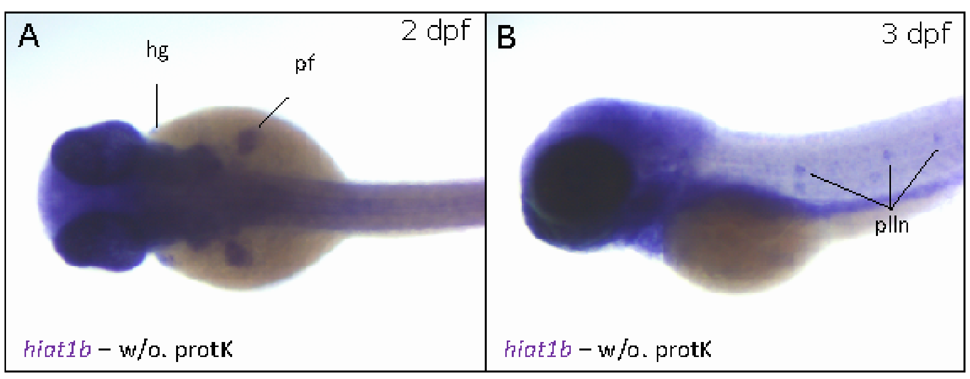

FIG S2

Fig. S2. *In situ* hybridization of DrHiat1b without proteinase K treatment. Additional staining for DrHiat1b can be detected in (B) the pectoral fin (pf) and weakly in the hatching gland (hg) at 2 days post fertilization (dpf), and in (C) the posterior lateral line neuromasts (plln) at 3 dpf. B, dorsal view, anterior to the left; C: lateral view, anterior to the left.

Table S1. Protein sequences for phylogenetic tree as shown in figure 1. Accession numbers are according to GenBank.

GenBank accession no.	Clusters as	Species	Common name	Class
NP 001085612.1	Hiat1b	*Xenopus laevis*	African clawed frog	Amphibia
XP 018114716.1	Hiat1-like	*Xenopus laevis*	African clawed frog	Amphibia
NP 001087834.1	Hiat1a	*Xenopus laevis*	African clawed frog	Amphibia
XP 002188818.1	Hiat1b	*Taeniopygia guttata*	Zebrafinch	Aves
XP 030113786.3	Hiat1-like	*Taeniopygia guttata*	Zebrafinch	Aves
XP 012426709.3	Hiat1a	*Taeniopygia guttata*	Zebrafinch	Aves
XP_041064351.1	Hiat1b	*Carcharodon carcharias*	Great white shark	Chondrichthyes
XP 041059808.1	Hiat1a	*Carcharodon carcharias*	Great white shark	Chondrichthyes
GCB60630.1	Hiat1b	*Scyliorhinus torazame*	Cloudy catshark	Chondrichthyes
GCB70945.1	Hiat1a	*Scyliorhinus torazame*	Cloudy catshark	Chondrichthyes
XP 033876203.1	Hiat1b	*Acipenser ruthenus*	Sterlet	Chondrostei
XP 034775964.1	Hiat1-like	*Acipenser ruthenus*	Sterlet	Chondrostei
XP 034767512.1	Hiat1a	*Acipenser ruthenus*	Sterlet	Chondrostei
DW250260.1	Hiat1	*Carcinus maenas*	Green crab	Crustacea
XP_032826511.1	Hiat1b	*Petromycon marinus*	Sea lamprey	Hyperoartia (Agnatha)
NP 149044.2	Hiat1b	*Homo sapiens*	Human	Mammalia
NP 115947.2	Hiat1-like	*Homo sapiens*	Human	Mammalia
NP 032272.2	Hiat1b	*Mus musculus*	House mouse	Mammalia
NP 001077370.1	Hiat1-like	*Mus musculus*	House mouse	Mammalia
XP 036707313.1	Hiat1b	*Balaenoptera musculus*	Blue whale	Mammalia (SW)
XP 036710915.1	Hiat1-like	*Balaenoptera musculus*	Blue whale	Mammalia (SW)
XP 039340654.1	Hiat1b	*Mauremys reevesii*	Chinese pond turtle	Reptilia (FW)
XP 039400711.1	Hiat1-like	*Mauremys reevesii*	Chinese pond turtle	Reptilia (FW)
XP 039371595.1	Hiat1a	*Mauremys reevesii*	Chinese pond turtle	Reptilia (FW)
XP 043347006.1	Hiat1b	*Dermochelys coriacea*	Leatherback sea turtle	Reptilia (SW)
XP 038258563.1	Hiat1-like	*Dermochelys coriacea*	Leatherback sea turtle	Reptilia (SW)
XP 038239659.1	Hiat1a	*Dermochelys coriacea*	Leatherback sea turtle	Reptilia (SW)
XP 013926066.1	Hiat1b	*Thamnophis sirtalis*	Common garter snake	Reptilia (T)
XP 013915054.1	Hiat1-like	*Thamnophis sirtalis*	Common garter snake	Reptilia (T)
XP 006000077.1	Hiat1b	*Latimeria chalumnae*	West Indian ocean coelacanth	Sarcopterygii
XP 006001415.1	Hiat1-like	*Latimeria chalumnae*	West Indian ocean coelacanth	Sarcopterygii
XP 014345977.1	Hiat1a	*Latimeria chalumnae*	West Indian ocean coelacanth	Sarcopterygii
XP 026091418.1	Hiat1b	*Carassius auratus*	Goldfish	Teleostei (FW)
XP 026076322.1	Hiat1-like	*Carassius auratus*	Goldfish	Teleostei (FW)
XP 026143900.1	Hiat1a	*Carassius auratus*	Goldfish	Teleostei (FW)
AAH97075.1	Hiat1b	*Danio rerio*	Zebrafish	Teleostei (FW)
XP 002663499.2	Hiat1-like	*Danio rerio*	Zebrafish	Teleostei (FW)
BC056817.1	Hiat1a	*Danio rerio*	Zebrafish	Teleostei (FW)
XP 014071494.1	Hiat1b	*Salmo salar*	Atlantik salmon	Teleostei (SW)
XP 013981624.1	Hiat1-like	*Salmo salar*	Atlantik salmon	Teleostei (SW)
XP 014047397.1	Hiat1a	*Salmo salar*	Atlantik salmon	Teleostei (SW)

Table S2. Primer sequences. Primers have been designed based on GenBank accession numbers XP_002663499.2 (DrHiat1-like), AAH97075.1 (DrHiat1a), and BC056817 (DrHiat1b).

Application	Name	Sequence (5'-3')	Amplicon size (bp)	Annealing temperature (°C)
ORF	DrHiat1a ORF forward	ACCATGACTGGAGAGAAAAAGAAGAAA	493	60
	DrHiat1a ORF reverse	TTATACGCTGTCCTCCAGTAA		
	DrHiat1b ORF forward	ACCATGACCCAGAAAAAGAAGAAGCGA	485	62
	DrHiat1b ORF reverse	TCAGACATTAGTGTCCTGAAGG		
Oocytes	DrHiat1a Xmal forward	TCCCCCCGGGACCATGACTGGAGAGAAAAAGAAGAAAA	513	65
	DrHiat1a XbaI reverse	GCTCTAGATTATACGCTGCTGTCCTCCAGTAAA		
	DrHiat1b Xmal forward	TCCCCCCGGGACCATGACCCAGAAAAAGAAGAAGCGAG	505	65
	DrHiat1b XbaI reverse	GCTCTAGATCAGACATTAGTGTCCTGTAGAAGG		
In situ	DrHiat1a insitu forward	AAAATCTAGAAACCATGACTGGAGAGAAAAAGAAGAAAA	513	65
	DrHiat1a insitu reverse	TTTTGGGCCCTACGCTGCTGTCCTCCAGTAAAGGC		
	DrHiat1b insitu forward	AAAATCTAGAACCATGACCCAGAAAAAGAAGAAGCGAG	505	65
	DrHiat1b insitu reverse	TTTTGGGCCCGACATTAGTGTCCTGTAGAAGGGGC		
Morpholinos	DrHiat1a MO forward	AAAAGAAGAAAAAGCGGCTGAAC	355	57
	DrHiat1a MO reverse	ACAGCAAACACTCCAGACATGG		
	DrHiat1b MO forward	ATTTCTGGAGTTCTTCGCTTGG	373	57
	DrHiat1b MO reverse	GACTGAGATACGCACCGATGG		